Comparison of diode-side-pumped Nd:YAG and Nd:YAP laser

Jan Šulc[a], Helena Jelínková[a], Jan K. Jabczyński[b]
Waldemar Żendzian[b], Jacek Kwiatkowski[b], Karel Nejezchleb[c], Václav Škoda[c]

[a]Czech Technical University, Faculty of Nuclear Sciences and Physical Engineering
Břehová 7, 115 19 Prague 1, Czech Republic
[b]Military University of Technology, Institute of Optoelectronics
Kaliskiego Str. 2, 00 908 Warsaw, Poland
[c]Crytur, Ltd. Turnov, Palackého 175, 511 01 Turnov, Czech Republic

ABSTRACT

Nd:YAG and Nd:YAP slab crystal in the form of triangle with the Brewster-angle-cut polished input faces was used as an active medium for diode-side-pumped laser. A horizontal projection of the active medium form is a triangle with 19.22 mm long base, 5 mm height, and thickness of 4 mm. This active crystal shape is one from the simplest form which makes possible to realise a slab side-pumped configuration with a total internal reflection. Optical pumping was accomplished by a quasi-cw diode ARR18P400 with peak power 400 W closely attached to the active crystal without any coupling optics. Both material were operated for most known Nd^{3+} ion transition ${}^4F_{3/2} \rightarrow {}^4I_{11/2}$ (1 μm) as well as for transition ${}^4F_{3/2} \rightarrow {}^4I_{13/2}$ which leads to the emission at 1.3 μm. The systems were tested in free running and Q switch regime. This system is enough compact to be useful tools for direct medical application.

Keywords: Nd:YAP, Nd:YAG, slab, Q-switching, LiF:F_2^-, V:YAG

1. INTRODUCTION

For the purpose of various applications (industry, medicine, military...) all-solid-state high-power and high-energy diode pumped laser systems are requested. The energy limit for these lasers is done primary by the active medium volume, active ions concentration and possibility of pumping. Significant influence on generated energy and mean power have also a heat sink possibilities required to dissipate heat generated in the active medium. The thermal gradients in the laser active medium are responsible for the optical and mechanical distortion which includes thermal focusing, stress induced biaxial focusing, and stress induced birefringence. These thermally induced effects degrade the optical quality of the active medium and limit the laser output mean power. One of the possibilities how decrease the unfavorable influence of the thermal gradients is proper choice of the active medium material, shape and heat sink geometry. From this reason many concepts of the solid-state active media form were proposed and experimentally investigated.[1] The cylindrical shape of the active medium can be, for the purpose of high energy and high mean power output, changed to a slab or disc concept. In the design of the slab the generated laser radiation can be directed along longitudinal axes of the active medium or along the "zig-zag" path – the laser beam traverses the slab using total internal reflection from the slab side faces.[2,3] All these systems were used for flashlamp pumping and similarly for diode pumping.[4,5] Especially for diode side pumped lasers various forms of the active media were used as for example triangle,[6] brick,[7,8] or pentagonal[9] shapes. The trigonal form of active medium follows the zig-zag slab system: it is slab with one internal reflection

Further author information: (Send correspondence to J.Š.)
J.Š.: E-mail: sulc@troja.fjfi.cvut.cz, Tel.: +420 221 912 240, Fax: +420 221 912 252
H.J.: E-mail: hjelin@troja.fjfi.cvut.cz, Tel.: +420 221 912 243, Fax: +420 221 912 252
J.J.: E-mail: jjabczynski@wat.edu.pl, Tel.: +48 226 859 678, Fax: +48 226 668 950
K.N.: E-mail: nejezchleb@crytur.cz, Tel.: +420 481 319 511, Fax: +420 481 322 323
V.Š.: E-mail: skoda@crytur.cz, Tel.: +420 481 319 511, Fax: +420 481 322 323

only. This arrangement is very convenient for diode side pumping and in comparison with brick system, the resonator with the trigonal active medium has convenient linear form.

In our previous work[10–12] the trigonal Nd:YAG slab crystal was used together with the $BaWO_4$ Raman crystal for generation of Stokes shifted laser radiation with wavelength 1170 nm. As continuation of this research, Nd:YAP triangle was prepared and the characterization of this material was performed in the same system together with the previously tested Nd:YAG crystal to compare this two materials.

2. MATERIALS AND METHODS

2.1. Laser Active Medium

As an active medium of constructed slab lasers two similar materials were compared: Nd doped YAG (yttrium aluminium garnet) and YAP (yttrium aluminium perovskite, also called YALO). In fact both of this matrices are from one physical-chemical system Y_2O_3–Al_2O_3 and also physical properties like melting point, hardness, thermal conductivity, etc. are quite similar.[13] The main difference between this two material is that cubic YAG is an isotropic crystal, while rhombic YAP crystal is anisotropic and its anisotropy is reflected also in its spectral properties. Thus Nd:YAP crystal orientation can be chosen for higher gain and low threshold or, alternatively, for low gain and high energy storage required for Q-switching.[14] Also it is well known that in the anisotropic material like Nd:YAP thermally-induced birefringence effects can be greatly reduced.[1]

Solid state lasers based on this materials are very common because of their simple construction, reliability and large variability. The main properties of this Nd-doped laser crystals are listed in Table 1. In this table corresponding laser channels for Nd^{3+} ion in both crystalline latices are noted to explain observed simultaneous dual wavelength emission corresponding with Nd^{3+} transition ${}^4F_{3/2} \rightarrow {}^4I_{13/2}$ in garnet.

Table 1. Comparison of Nd^{3+}:YAP & Nd^{3+}:YAG chosen physical properties.

	Nd:YAG	Nd:YAP	*Note*
Full name	Neodymium doped yttrium aluminium garnet	Neodymium doped yttrium aluminium perovskite	
Chemical formula	$Nd^{3+}:Y_3Al_5O_{12}$	$Nd^{3+}:YAlO_3$	
	Isotropic medium	Anisotropic medium	
Refractive index ($\lambda = 1.06\,\mu$m)	$n = 1.816$	$n_a = 1.929$ $n_b = 1.943$ $n_c = 1.952$	*Ref.*[13]
Thermal conductivity	$0.13\,\mathrm{W.cm^{-1}.K^{-1}}$	$0.11\,\mathrm{W.cm^{-1}.K^{-1}}$	*Ref.*[13]
Nd^{3+} doping level	1 at. %	1 at. %	*Producer data*
Pumping wavelength	808 nm	803 nm	
Absorption coefficient	$4.3\,\mathrm{cm^{-1}}$ (@ 808 nm)	$4.8\,\mathrm{cm^{-1}}$ (@ 803 nm)	*Measured*
Lifetime at level ${}^4F_{3/2}$	$258 \pm 3\,\mu$s	$156 \pm 1\,\mu$s	*Measured*
Laser transition ${}^4F_{3/2} \rightarrow {}^4I_{11/2}$	$\lambda = 1064.2$ nm ($\sigma_e \sim 71 \times 10^{-20}\,\mathrm{cm^2}$)	$\lambda = 1064.6$ nm ($\sigma_e \sim 17 \times 10^{-20}\,\mathrm{cm^2}$, $\mathbf{k}\|\mathbf{c}$)	*Ref.*[13, 15]
	$\lambda = 1077.9$ nm ($\sigma_e \sim 12 \times 10^{-20}\,\mathrm{cm^2}$)	$\lambda = 1079.6$ nm ($\sigma_e \sim 46 \times 10^{-20}\,\mathrm{cm^2}$, $\mathbf{k}\|\mathbf{b}$)	
Laser transition ${}^4F_{3/2} \rightarrow {}^4I_{13/2}$	$\lambda = 1318.4$ nm ($\sigma_e \sim 15 \times 10^{-20}\,\mathrm{cm^2}$)	$\lambda = 1317.5$ nm ($\sigma_e \sim 0.5 \times 10^{-20}\,\mathrm{cm^2}$, $\mathbf{k}\|\mathbf{c}$)	*Ref.*[13, 15, 16]
	$\lambda = 1338.1$ nm ($\sigma_e \sim 15 \times 10^{-20}\,\mathrm{cm^2}$)	$\lambda = 1341.6$ nm ($\sigma_e \sim 22 \times 10^{-20}\,\mathrm{cm^2}$, $\mathbf{k}\|\mathbf{b}$)	

2.1.1. Active Medium Geometry

The active medium in the form of isosceles triangle was used. Dimensions of tested Nd:YAG and Nd:YAP crystal cuts are evident form Figures 2 and 1. It is seen that the dimensions of tested samples are not exactly the same. The main difference is in thickness of crystals (Nd:YAP crystal is about 1 mm thicker than Nd:YAG crystal). Sideways paths of triangle are polished and by these sides propagates the generated radiation. The oscillating laser radiation is entering into the crystal under Brewster angle, so the horizontal part of the polarization is travelling without losses.

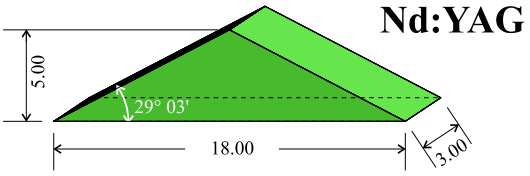

Figure 1. Diagram of the Nd:YAG triangle crystal dimensions.

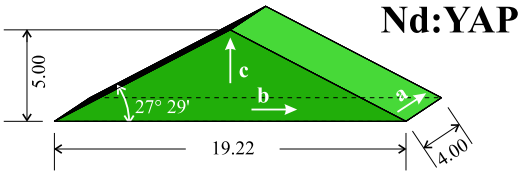

Figure 2. Diagram of the dimensions and crystallographic orientation of Nd:YAP triangle crystal.

The horizontally polarized pumping radiation is entering into the crystal through the basis of triangle (Figure 3). In Nd:YAP crystal the propagation of pumping radiation corresponds with **c**-direction. The pumping radiation is absorbed in the laser crystal in the place of internal total reflection of generated laser beam. Some part of the pumping radiation (10 %) is reflected back from the uncoated crystal-air boundary. It has to be noted, that due to zig-zag propagation of the laser radiation through the slab crystal, the radiation way is not exactly paralel to the crystallographic **b**-direction and the value of laser emission cross-section σ_e in Table 1 should be decreased for Nd:YAP crystal.

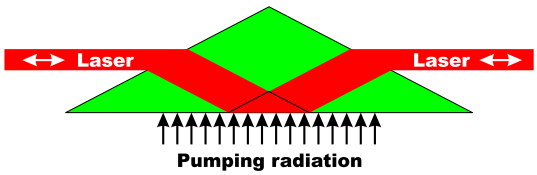

Figure 3. Laser radiation pass by triangle crystal.

2.2. Pumping System

For active medium pumping, a quasi-CW laser diode (QCW-LD) ARR18P400 (*Cutting Edge Optronics*) was used. The diode light emission area with dimensions 10×3 mm consists of 8 linear bars. Maximum output power of this diode was 400 W. The diode was cooled by Peltier cooling system with the maximum cooling power 120 W. The power supply used for this diode was LDI-928 driver with the maximum peak current 150 A. The maximum current was set at 55 A. The length of pumping pulse was set to 250 μs which yields to the maximum pumping energy 100 mJ. Repetition rate of the pumping diode was set on 20 Hz. The operating wavelength was tuned by changing of laser diode temperature: for temperature 15 °C laser diode operates at at 803 nm, wavelength 808 nm corresponds with temperature 35 °C. The line-width of emitted radiation was ~ 3 nm.

2.3. Laser Oscillator

The side-pumped trigonal crystals were for most cases tested in simple semi-concave cavity. This cavity was created by one plan dielectric rear mirror (RM) with reflectivity 100 % for operating wavelength, and one dielectric spherical mirror with radius of curvature larger than the length of the cavity. This mirror serves as an output coupler (OC). The laser crystal was placed close to this mirror because of higher mode volume in this place. This basic arrangement of the laser resonator is shown on Figure 4.

The laser operation was tested in sequence at two main Nd^{3+} ion laser transitions ${}^4F_{3/2} \rightarrow {}^4I_{11/2}$, and ${}^4F_{3/2} \rightarrow {}^4I_{13/2}$ corresponding with emission in 1 μm and 1.3 μm spectral range, respectively. For this reason

two different sets of various mirrors were used. First set designate for laser operation at wavelength around 1 μm consist of one flat 100 % reflecting RM and of three OC with reflectivities and 98 %, 93 % and 92 %, and curvatures 500 mm, infinity and 100 mm, respectively. Second set designate for laser operation at wavelength around 1.3 μm consist also of one flat 100 % reflecting RM, and next of one OC with reflectivity 97.5 % and radius 500 mm, and of five mirrors with radius of curvature 146 mm and with reflectivities 97.5 %, 94.5 %, 92.7 %, 89.2 %, and 88.1 %.

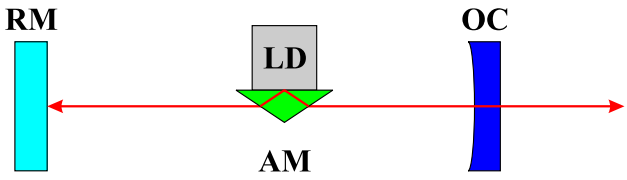

Figure 4. Basic arrangement of the laser resonator with side-pumped trigonal crystal (LD – laser pumping diode, AM – active medium, OC – laser output coupler, RM – laser rear mirror).

2.4. Saturable Absorbers

For the Q-switching at 1 μm spectral region (Nd^{3+} transition ${}^4F_{3/2} \rightarrow {}^4I_{11/2}$) the color center crystal[17] LiF:F_2^- was inserted into the laser resonator composed from the plane rear mirror and output coupler with reflectivity 92 % and with the radius 500 mm. The diagram of the setup is shown in Figure 5. The initial transmission of the saturable absorber crystal was 60 % including Fresnell losses (no AR coatings were applied on this crystal).

For the Q-switching at 1.3 μm spectral region two samples of V:YAG crystals[18] with different initial transmission were used. The diameter of used discs was 7 mm and the thickness was 235 μm, and 320 μm. Corresponding initial transmission of used V:YAG crystal samples was 96 %, and 93 %. These discs were both sides polished and AR/AR coated to obtain a minimum reflectivity on 1.08 and 1.34 μm. Crystals were fixed in adjustable air-cooled cupreous ring and placed in the laser resonator close to the resonator focus (Figure 5).

Figure 5. Arrangement of Q-switched laser with of side-pumped active medium (LD – laser pumping diode, AM – active medium, OC – curved laser output coupler, RM – flat laser rear mirror, SA – saturable absorber).

2.5. Measuring Instruments

For measurement of the laser radiation output energy the *Molectron* probe J25 (voltage responsivity 8.59 V/J) was used. To investigate the length of generated giant pulse *Tektronix* oscilloscope (TDS 3052, 500 MHz) with the silicon PIN photodiode HP 4207 (for 1 μm spectral region) or InGaAs photodiode (for 1.3 μm spectral region) was used. The spectrum of the laser radiation in 1 μm range was investigated by *Oriel* monochromator 77250 and it was recorded by the CCD camera EDC-1000HR (resolution 753 × 244). The spectrum of the generated radiation in range 1.3 μm was investigated with the help of an IR wavelength meter *StellarNet* EPP 2000. The mentioned CCD camera was also used for laser beam spatial structure in 1 μm spectral range.

3. RESULTS

3.1. Free-running regime

The trigonal Nd:YAG and Nd:YAP slab crystals were tested in QCW-LD side-pumped laser with simple semi-concave cavity described in section 2.3 – see Figure 6. The laser operation on two Nd^{3+} ion transition was proved, emission wavelength was measured, and optimized laser resonator configuration was found for both corresponding spectral ranges. Results are summarized in next subsections.

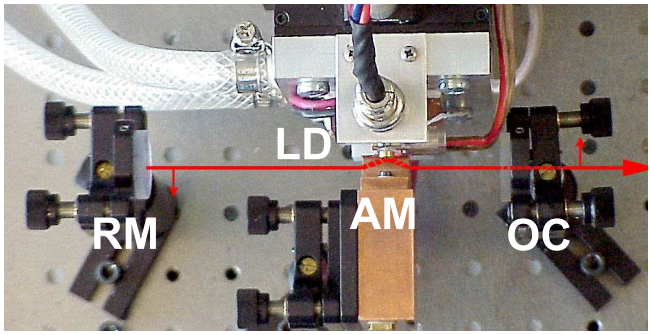

Figure 6. Photo of the laser oscillator arrangement with the side-pumped trigonal active medium. The laser resonator length is 130 mm (LD – laser pumping diode, AM – active medium in holder, OC – laser output coupler, RM – laser rear mirror).

3.1.1. Laser operation at Nd^{3+} transition $^4F_{3/2} \rightarrow {}^4I_{11/2}$

Efficient generation at Nd^{3+} iont transition $^4F_{3/2} \rightarrow {}^4I_{11/2}$ was achieved for both side-pumped trigonal slab Nd:YAG and Nd:YAP crystal. Corresponding commonly known wavelengths are 1064.2 nm (Nd:YAG) and 1079.6 nm (Nd:YAP). For each crystal proper pumping wavelength was used (see Table 1). Laser output radiation was polarized horizontally which agree with the minimal losses of the active medium Brewster faces. For both crystals several mirrors and resonator configurations were tested and laser optimization was made. The output characteristic for the best configuration of the output coupler and pumping is shown in Figure 7 and 8.

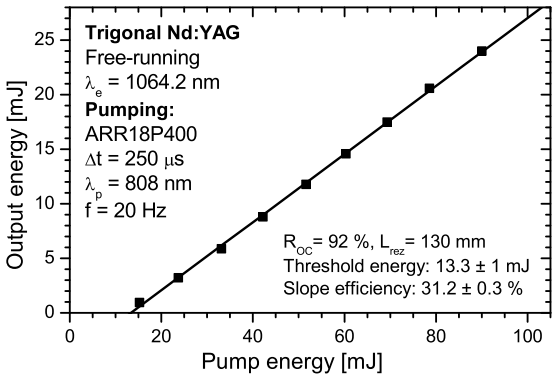

Figure 7. Dependence of the Nd:YAG slab triangle output energy on pumping energy for the case of generation at $\lambda = 1064.2$ nm.

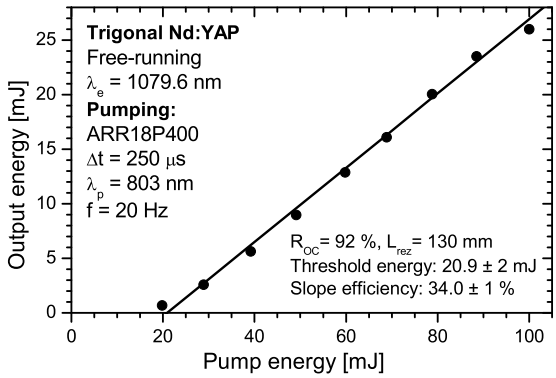

Figure 8. Dependence of the Nd:YAP slab triangle output energy on pumping energy for the case of generation at $\lambda = 1079.6$ nm.

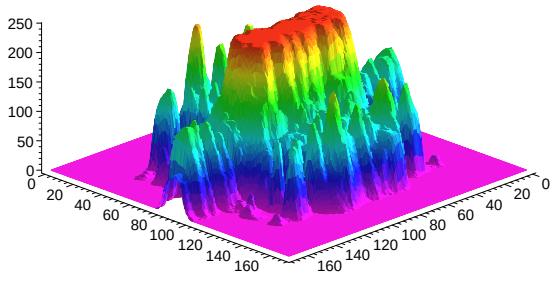

Figure 9. Nd:YAG side pumped laser beam profile 80 mm from output coupler (in horizontal plane 100 units $\equiv$ 2.5 mm, vertical axis is $\propto$ intensity).

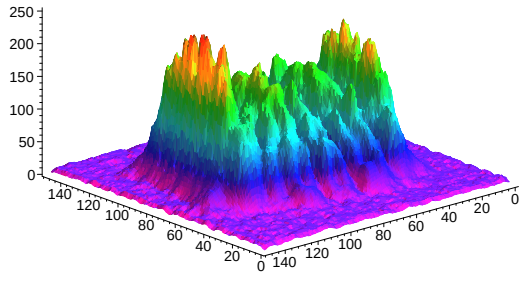

Figure 10. Nd:YAP side pumped laser beam profile 80 mm from output coupler (in horizontal plane 100 units $\equiv$ 2.5 mm, vertical axis is $\propto$ intensity).

Analyzing the space profile of the laser beam in several distances from resonator output coupler it was found that both Nd:YAG and Nd:YAP laser beam parameter $M^2 \sim 32$. The beam profile o Nd:YAG and Nd:YAP laser is shown in Figure 9 and 10.

3.1.2. Laser operation at Nd^{3+} transition $^4F_{3/2} \rightarrow {}^4I_{13/2}$

In the next step, the laser resonator mirrors were changed to obtained laser emission at the $^4F_{3/2} \rightarrow {}^4I_{13/2}$ transition. This Nd^{3+} ion transition corresponds with the generation of radiation in 1.3 μm spectral range. Corresponding wavelengths are 1318.4 nm (Nd:YAG) and 1341.6 nm (Nd:YAP). Measured spectral lines for both materials are shown in Figure 11 and 12. Figure 11 shows that emission of Nd:YAG crystal contains both radiation at wavelength 1318.4 nm and 1338.1 nm.

Also for the side-pumped Nd:YAG and Nd:YAP laser operating at transition $^4F_{3/2} \rightarrow {}^4I_{13/2}$ output characteristics in free-running regime were measured in dependence of laser resonator parameters. The output characteristic for the optimal configuration of the output coupler and pumping is shown in Figure 13 and 14.

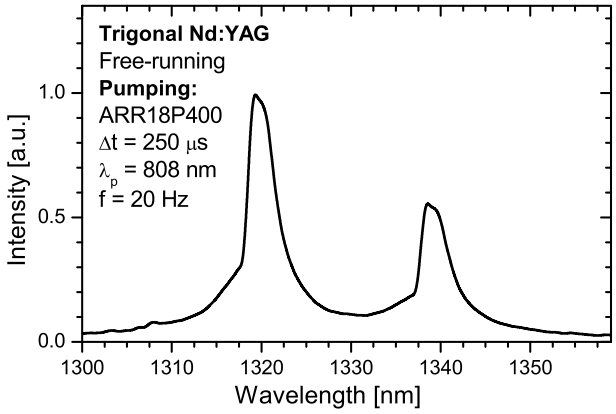

Figure 11. Spectrum of free-running Nd:YAG laser emission corresponding to operation at Nd^{3+} transition $^4F_{3/2} \rightarrow {}^4I_{13/2}$.

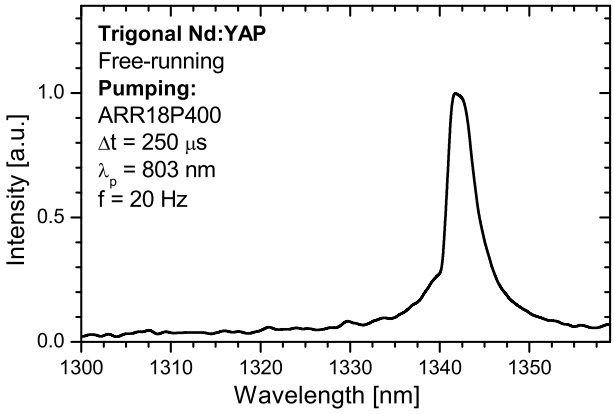

Figure 12. Spectrum of free-running Nd:YAP laser emission corresponding to operation at Nd^{3+} transition $^4F_{3/2} \rightarrow {}^4I_{13/2}$.

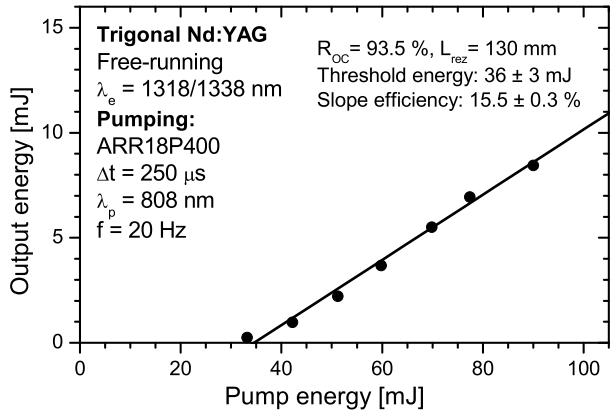

Figure 13. Dependence of the Nd:YAG slab triangle output energy on pumping energy for the case of generation at $\lambda = 1318.4\,(1338.1)$ nm.

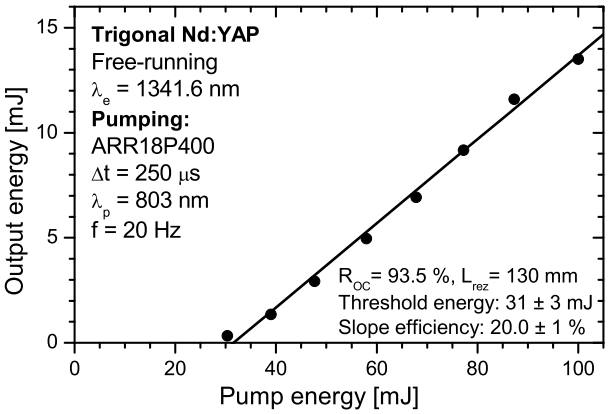

Figure 14. Dependence of the Nd:YAP slab triangle output energy on pumping energy for the case of generation at $\lambda = 1341.6$ nm.

3.2. Q-switching regime

On the base of the trigonal Nd:YAG and Nd:YAP side-pumped slab crystals Q-switched laser were also realized. Generation of giant pulses in wavelength range around 1 μm and 1.3 μm were achieved. Used resonator configuration and saturable absorbers were described in section 2.4. Results are summarized in next subsections.

3.2.1. Laser operation at Nd^{3+} transition $^4F_{3/2} \rightarrow {}^4I_{11/2}$

For Q-switching in 1 μm spectral range the above described LiF:F_2^- saturable absorber ($T_0 = 60\,\%$) was inserted into the laser resonator composed from the plane rear mirror and output coupler with reflectivity 92 % and with the radius 500 mm. The diagram of the setup is shown in Figure 5. The stable output generation was obtained for the input energy 100 mJ. In case of side-pumped Nd:YAG crystal, the length and the energy of the generated giant pulse was 36 ns (FWHM) (Figure 15) and 960 μJ, respectively. The corresponding peak power of the output radiation at wavelength 1064.2 ns was approximately equal 20 kW. With side-pumped Nd:YAG crystal we have obtained giant pulse 70 ns long (FWHM) (Figure 16) with energy 2 mJ (output peak power $\sim$ 30 kW) at wavelength 1079.6 ns.

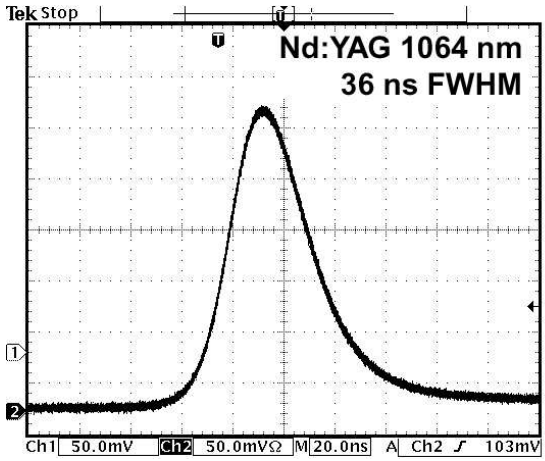

Figure 15. Q-switched side-pumped Nd:YAG laser operating at 1064.2 nm. Oscillograph of generated radiation (20 ns/div).

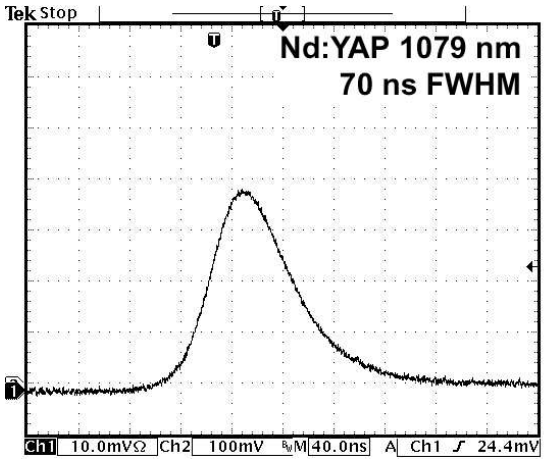

Figure 16. Q-switched side-pumped Nd:YAP laser operating at 1079.6 nm. Oscillograph of generated radiation (40 ns/div).

3.2.2. Laser operation at Nd^{3+} transition $^4F_{3/2} \rightarrow {}^4I_{13/2}$

The passive Q-switching at Nd^{3+} transition $^4F_{3/2} \rightarrow {}^4I_{13/2}$ was achieved placing of the V:YAG crystal into the 160 mm long laser resonator composed from the plane rear mirror and output coupler with reflectivity 97.5 % (radius 500 mm). V:YAG crystal with initial transmission $T_0 = 96\,\%$ was used and giant pulse generation was obtained for both Nd:YAG and Nd:YAP crystal. In both cases the length and the energy of the generated giant pulse was approximately the same – 105 ns (FWHM) (see Figures 17 and 18). Generated pulse energies was also similar: 460 μJ for Nd:YAG and 560 μJ for Nd:YAP. The corresponding peak power of the output radiation was equal 4.4 kW and 5.5 kW, respectively.

With side-pumped Nd:YAG crystal we have also obtained giant pulse 72 ns long (FWHM) using thicker ($T_0 = 93\,\%$) V:YAG crystal (Figure 19) with energy 530 μJ (output peak power $\sim$ 7.4 kW). It is important to note than for both V:YAG crystals the emission from the Q-switched Nd:YAG laser was observed only at wavelength 1338.1 nm like illustrates spectrum at Figure 20. This emission spectra of Nd:YAG laser Q-switched by V:YAG crystal is done by V:YAG absorption maximum which is situated closer to 1318 nm line.

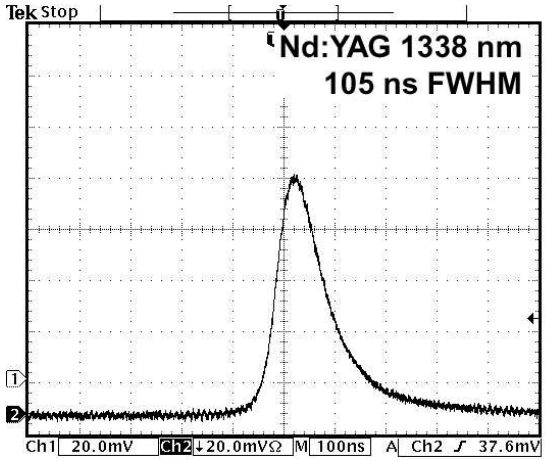

Figure 17. Q-switched side-pumped Nd:YAG laser operating at 1338.1 nm (saturable absorber initial transmission $T_0 = 96\,\%$). Oscillograph of generated radiation (100 ns/div).

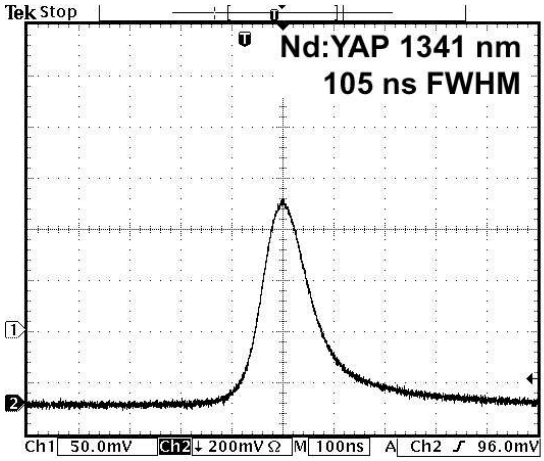

Figure 18. Q-switched side-pumped Nd:YAP laser operating at 1341.6 nm (saturable absorber initial transmission $T_0 = 96\,\%$). Oscillograph of generated radiation (100 ns/div).

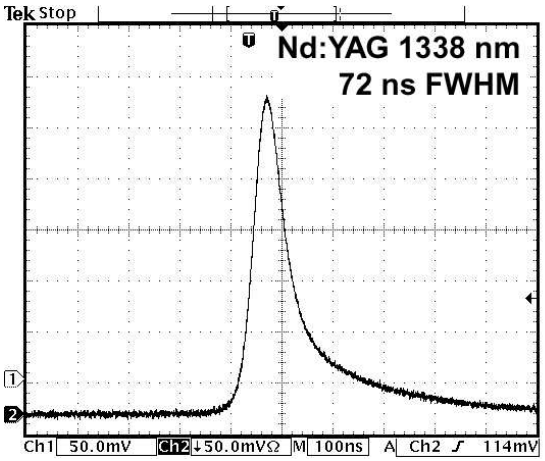

Figure 19. Q-switched side-pumped Nd:YAG laser operating at 1338.1 nm (saturable absorber initial transmission $T_0 = 93\,\%$). Oscillograph of generated radiation (100 ns/div).

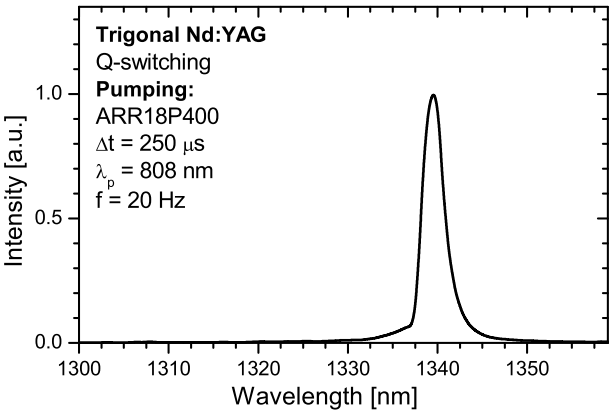

Figure 20. Q-switched side-pumped Nd:YAG laser operating at 1338.1 nm (saturable absorber initial transmission $T_0 = 93\,\%$). Spectrum of generated radiation.

4. DISCUSSION

With the goal of obtaining higher energy in the single mid-infrared pulse from compact cheap laser system, the laser with side-pumped trigona active medium was realized. For side pumping the quasi-CW laser diode ARR18P400 with the maximum peak power 400 W was used. The diode had not any collimation optic and the pumping radiation was not concentrated. As an active medium trigonal Nd:YAG and Nd:YAP crystal was tested.

The laser emission at the wavelength range 1 μm or 1.3 μm in free-running regime was reached with both side-pumped trigonal crystals. Results are summarized in Table 2. It is obvious that in free-running regime the threshold energy E_{th} is mainly affected by stimulated emission cross-section σ_e. From a simple free-running laser analysis it follows, that for two systems with similar pumping efficiency and laser resonator parameters (passive and active losses) should be:

$$\frac{E_{th}^A}{E_{th}^B} \approx \frac{\sigma_e^B}{\sigma_e^A}. \tag{1}$$

Obtained results fulfill this condition well for both 1 μm and 1.3 μm emission range (compare last two in Table 2) an small divergencies can be explained as en effect of zig-zag laser beam propagation trough the active medium (see section 2.1.1). It means that parameters like losses and energy conversion efficiency are similar for both crystals and the main difference is done by value of emission cross-section coefficient. Because higher emission cross-section coefficient means lower threshold, than for operation at 1 μm spectral region Nd:YAG is better and for operation at 1.3 μm Nd:YAP crystal should be used. The observed higher slope efficiency obtained with Nd:YAP crystal in both spectral ranges can be explained as an effect of multimode emission from crystal with higher volume – tested Nd:YAP trigonal crystal was about 1 mm thicker than Nd:YAG crystal.

Table 2. Results obtained with Nd^{3+}:YAP and Nd^{3+}:YAG side-pumped trigonal crystals in free-running regime.

Crystal	Emission [nm]	σ_e [cm^2]	Output coupler	E_{th} [mJ]	Slope efficiency	$E_{th}^{YAP}/E_{th}^{YAG}$	$\sigma_e^{YAG}/\sigma_e^{YAP}$
Nd:YAG	1064.2	71×10^{-20}	92.0 %	13.3	21.2 %	1.57	1.54
Nd:YAP	1079.6	46×10^{-20}	92.0 %	20.9	34.0 %		
Nd:YAG	1318.1	15×10^{-20}	93.5 %	36.0	15.5 %	0.86	0.68
Nd:YAP	1341.6	22×10^{-20}	93.5 %	31.0	20.0 %		

From the results obtained in Q-switch regime it can be summarized, lower threshold and longer lifetime it is possible for the same maximum pump energy obtained shorter pulses with Nd:YAG active medium. Nevertheless, the results obtained with Nd:YAP crystal ware comparable and with proper pumping beam quality should be better.

5. CONCLUSION

Trigonal Nd:YAG and Nd:YAP slabs were tested as an active medium for diode-side-pumped laser. The laser emission was achieved with both crystals at spectral region around 1 μm and 1.3 μm in free-running and Q-switched regime. From the comparison it follows that except for the free-running emission at 1.3 μm Nd:YAG crystal is slightly better than Nd:YAP. Nevertheless, both systems are enough compact to be used as a tool for medical application.

6. ACKNOWLEDGEMENTS

This research has been supported by the Grant of the Czech Ministry of Industry and Trade No. FF-P/125, and by the Czech AIP grant *Development and investigations of pulsed solid state lasers* No. 58.

REFERENCES

1. W. Koechner, *Solid state laser engeniering*, Springer-Verlag, Berlin, 5th ed., 1999.
2. W. S. Martin and J. P. Chernoch. US Patent No. 3, 633, 126, Jan. 1972.
3. J. P. Chernoch, W. S. Martin, and J. C. Almasi, "Performance characteristics of a face-pumped, face-cooled laser, the mini-FPL," Technical Report AFAL-TR-71-3, Air Force Avionics Lab., Wright Patterson AFB, Ohio, 1971.
4. A. Agnesi, F. Pirzio, A. Tomaselli, F. Bonfigli, and T. Marolo, "Thermal lens characterization of a side-pumped bounce geometry Nd:YVO_4 laser," in *XV Internal.Symposium on Gas Flow and Chemical Laser & High Power Laser Konference*, *Book of abstract*, pp. 114 (P1–10), (Prague, Czech Republic), Aug. 2004.
5. T. S. Rutherford, W. M. Tulloch, S. Sinha, and R. L. Byer, "Yb:YAG and Nd:YAG edge-pumped slab lasers," *Optics Letters* **26**, pp. 986–988, July 2001.
6. W. Żendzian, J. K. Jabczyński, and Z. Mierczyk, "Investigation on passively Q-switched Nd:YAG slab laser pumped by 2D quasi cw diode laser stack," *Opto-electronics Review* **9**, pp. 75–81, July 2001.

7. J. E. Bernard and A. J. Alcock, "High-efficiency diode-pumped Nd:YVO_4 slab laser," *Optics Letters* **18**, pp. 968–970, June 1993.
8. J. K. Jabczyński, J. Kwiatkowski, and W. Żendzian, "Optical characterization of diode side pumped active elements," in *13th Polish-Czech-Slovak Conference on Wave and Quantum Aspects of Contemporary Optics*, J. Nowak, M. Zajac, and J. Masajada, eds., *Proceedings of SPIE* **5259**, pp. 296–302, Nov. 2003.
9. C. Ziolek, H. Ernst, G. F. Will, H. Lubatschowski, H. Welling, and W. Ertmer, "High-repetition-rate, high-average-power, diode-pumped 2.94-μm Er:YAG laser," *Optics Letters* **26**, pp. 599–601, May 2001.
10. P. Černý, W. Żendzian, J. K. Jabczyński, H. Jelínková, J. Šulc, *et al.*, "Efficient diode-pumped passively Q-switched raman laser on barium tungstate crystal," *Optics Communications* **209**(4–6), pp. 403–409, 2002.
11. H. Jelínková, P. Černý, W. Żendzian, J. K. Jabczyński, and J. Šulc, "Compact diode-pumped Nd:YAG/$BaWO_4$ raman laser," in *IEEE/LEOS Annual Meeting 2002*, *Conference Proceedings*, p. 451, Institute of Electrical and Electronic Engineers, (Piscataway), 2002.
12. H. Jelínková, P. Černý, J. Šulc, J. K. Jabczyński, and W. Żendzian, "Diode pumped passively Q-switched nanosecond raman laser on $BaWO_4$ crystal converter," in *Photonics, Devices, and Systems II.*, M. Hrabovsky, D. Senderakova, and P. Tomanek, eds., *Proceedings of SPIE* **5036**, pp. 582–587, SPIE, (Prague, Czech Republic), July 2003.
13. A. A. Kaminskii, *Laser crystals. Their physics and properties*, no. 14 in Springer series in optical sciences, Springer-Verlag, Berlin, 1981.
14. H. Y. Shen, G. Zhang, C. H. Huang, R. R. Zeng, and M. Wei, "High power 1341.4 nm Nd:$YAlO_3$ CW laser and its performances," *Optics & Laser Technology* **35**, pp. 69–72, 2003.
15. S. Singh, R. G. Smith, and L. G. Van Uitert, "Stimulated-emission cross section and fluorescent quantum efficiency of Nd^{3+} in yttrium aluminum garnet at room temperature," *Physical Review B* **10**, pp. 2566–2572, Sept. 1974.
16. H. Shen, T. Lian, R. Zheng, Y. Zhou, G. Yu, C. Huang, H. Liao, and Z. Zheng, "Measurement of the stimulated emission cross section for the $^4F_{3/2}$ - $^4I_{13/2}$ transition of Nd^{3+} in $YAlO_3$ crystal," *IEEE Journal of Quantum Electronics* **25**, pp. 144–146, Feb. 1989.
17. N. N. Ilichev, A. V. Kiryanov, and P. P. Pashinin, "Experimental and theoretical study of a neodymium laser passively Q-switched with doped crystals LiF:F_2^- and Cr^{4+}:YAG: an influence of nonlinear absorption anisotropy in the switches on output parameters," in *OPTIKA '98: 5th Congress on Modern Optics*, G. Akos, G. Lupkovics, and A. Podmaniczky, eds., *Proceedings of SPIE* **3573**, pp. 10–12, Aug. 1998.
18. J. K. Jabczyński, K. Kopczyński, Z. Mierczyk, A. Agnesi, A. Guandalini, and G. Reali, "Application of V^{3+}:YAG crystals for Q-switching and mode-locking of 1.3-μm diode-pumped neodymium lasers," *Optical Engineering* **40**, pp. 2802–2811, Dec. 2001.